Experimental investigation of partial synchronization in coupled chaotic oscillators

Ismael A. Heisler, Thomas Braun, Ying Zhang, Gang Hu, and Hilda A. Cerdeira

Citation: Chaos: An Interdisciplinary Journal of Nonlinear Science **13**, 185 (2003); doi: 10.1063/1.1505811
View online: http://dx.doi.org/10.1063/1.1505811
View Table of Contents: http://scitation.aip.org/content/aip/journal/chaos/13/1?ver=pdfcov
Published by the AIP Publishing

Experimental investigation of partial synchronization in coupled chaotic oscillators

Ismael A. Heisler and Thomas Braun
Instituto de Física, Universidade Federal do Rio Grande do Sul, Caixa Postal 15051, 91501-970 Porto Alegre, RS, Brazil

Ying Zhang
Chinese Center for Advanced Science and Technology (World Laboratory), Beijing 8730, China and The Abdus Salam International Centre for Theoretical Physics, P.O. Box 586, 34100 Trieste, Italy

Gang Hu
Chinese Center for Advanced Science and Technology (World Laboratory), Beijing 8730, China and Department of Physics, Beijing Normal University, Beijing 100875, China

Hilda A. Cerdeira
The Abdus Salam International Centre for Theoretical Physics, P.O. Box 586, 34100 Trieste, Italy

(Received 16 April 2002; accepted 14 July 2002; published 21 February 2003)

The dynamical behavior of a ring of six diffusively coupled Rössler circuits, with different coupling schemes, is experimentally and numerically investigated using the coupling strength as a control parameter. The ring shows partial synchronization and all the five patterns predicted analyzing the symmetries of the ring are obtained experimentally. To compare with the experiment, the ring has been integrated numerically and the results are in good qualitative agreement with the experimental ones. The results are analyzed through the graphs generated plotting the y variable of the ith circuit versus the variable y of the jth circuit. As an auxiliary tool to identify numerically the behavior of the oscillators, the three largest Lyapunov exponents of the ring are obtained. © *2003 American Institute of Physics.* [DOI: 10.1063/1.1505811]

Synchronization of coupled nonlinear systems is ubiquitous in nature. It has been observed in physical, chemical, ecological, physiological systems among others. In spite of these interesting results, very few experiments have been done to explore the full complexity of this issue. Synchronization is considered as the complete coincidence of the states of the individual coupled identical systems regardless whether this state is periodic or chaotic. Besides this full synchronization, it has been realized that also partial synchronization may occur, i.e., some of the systems synchronize with each other and others do not. When the systems are not globally coupled but in a local manner as, for instance, through its nearest neighbors, the partial synchronization is observed in terms of spatial patterns. The symmetry of the coupling determines the possible spatial synchronization patterns. Different patterns may be obtained changing the coupling strength. Thus due to the simultaneous presence of a temporal chaotic behavior and spatial patterns, the arrangement of locally coupled systems is well suited for the study of spatio-temporal complexity.

I. INTRODUCTION

Synchronization in chaotic coupled systems has been the focus of recent research. Different systems have been studied in the search of models of spatiotemporal chaotic behavior in a large range of systems in physics, biology, chemistry, physioneurology, etc. It has been well known that these systems synchronize since the early work of Heagy *et al.*,[1] but it was only recently that spatio-temporal coherent patterns were found not only when the single oscillators are in the periodic state, but also chaotic. Recently we looked at a ring of chaotic Rössler oscillators, and we showed that it presents partial synchronization, with a series of stable patterns static as well as dynamic, such as a rotating wave.[2,3] In particular, we had proposed to ourselves to look for all the symmetries associated with a group of six oscillators in a ring, which have been discussed amply in the literature for the case of periodic motion.[4–7] Belykh *et al.*[8] studied the stability of partially synchronous oscillations of diffusive coupled dynamical systems. They investigated the instabilities of the synchronization manifold and showed that they were due to the existence of transverse stable manifolds which will give rise to the appearance of partial synchronization. Even when the problem is essentially the same, there is a clear difference in their approach and ours. While we had assumed that a pattern, determined by group theoretical analysis, exists, search for it, and study its stability, Belykh *et al.* had looked for the possibility of having partial synchronization, as a breakdown of the stability of the full synchronization manifold, which give rise to stable transverse manifolds.

The success of these results prompts us to look for an experimental setup with the same conditions where we could search for the patterns that we had predicted. In this work we present it and analyze it numerically. In Sec. II, we discuss the notion of partial synchronization and the patterns available for the system under consideration. In Sec. III we

present the experimental setup. In Sec. IV we compare and discuss the experimental and the numerical results, and in Sec. V we present the conclusions.

II. PARTIAL SYNCHRONIZATION

Let us consider a system of N Rössler oscillators, placed on a ring with nearest neighbors diffusive couplings, given by

$$\frac{dx_i}{dt} = -(y_i + z_i) + \epsilon(x_{i-1} + x_{i+1} - 2x_i),$$

$$\frac{dy_i}{dt} = x_i + ay_i + \epsilon(y_{i-1} + y_{i+1} - 2y_i),$$

$$\frac{dz_i}{dt} = b + z_i(x_i - c) + \epsilon(z_{i-1} + z_{i+1} - 2z_i),$$

$$x_{N+1} = x_1, \quad y_{N+1} = y_1, \quad z_{N+1} = z_1. \tag{1}$$

A simple analysis based on the topology of the structure shows that a system of N oscillators on a ring has the following symmetries: (a) it is invariant to the exchange between clockwise and counterclockwise direction due to the symmetric coupling, (b) Eq. (1) satisfies spatial permutational symmetries, i.e., they are invariant under the exchange $r_i \Leftrightarrow r_j$. Any breaking from these symmetries must happen spontaneously.[2]

We shall restrict our discussion to the case of six oscillators placed on a ring in the order of $i = 1,2,3,4,5,6$ with 7 being identical to 1, each place on the ring oscillates with a given power spectrum, which we call state. There are $m = 6$ possible states. In Ref. 9 we studied the possible arrangements or patterns[4] and their stability, and established that the possible partially synchronized states are:

$m = 1$: it corresponds to full synchronization, it has been given extensive attention in the literature.[1,10–13]

$m = 2$: in this case the six oscillators divide into two clusters, where a cluster is defined by a subset with n elements with $r_i(t) = r_j(t)$, for i and j in the same cluster. Representing one cluster state by a and the other by b, there are two and only two topologically distinct patterns: $\{ababab\}$ and $\{aabaab\}$.

$m = 3$: in this case there are also only two allowed patterns: $\{abbacc\}$ and $\{abcabc\}$.

$m = 4$: there is only one partially synchronized state, $\{abcbad\}$.

There is no pattern for $m = 5$, for a system of six oscillators, and $m = 6$ corresponds to the case when all oscillators behave independently. Their instabilities are determined by the largest Lyapunov exponent transverse to the corresponding partially synchronized manifold.

In the abovementioned reference[9] we made an exhaustive study proving the existence and the stability of those symmetries for a system of Rössler oscillators. Later on we also showed that a rotating wave, a spatio-temporal pattern predicted by group theoretical analysis in single oscillator-periodic state, also exists in chaotic systems.[3] In the next section we present measurements performed on a system of oscillators, which we shall compare with numerical predictions in Sec. IV.

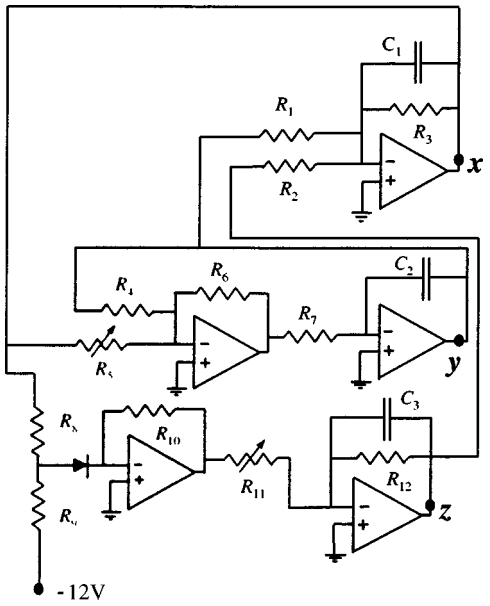

FIG. 1. Experimental setup for a single Rössler oscillator. We chose $C_1 = C_2 = C_3 = 220$ pF and $R_1 = 100$ kΩ, $R_2 = 200$ kΩ, $R_3 = 2$ MΩ, $R_4 = 75$ kΩ, $R_6 = 10$ kΩ, $R_7 = 100$ kΩ, $R_8 = 10$ kΩ, $R_9 = 68$ kΩ, $R_{10} = 150$ kΩ, and $R_{12} = 100$ kΩ. R_5 and R_{11} are variable resistors, their values are adjusted to obtain different outputs from the circuit. The diode is a BA316 and the operational amplifiers are TL072. The resistors have 1% tolerance and the capacitors have 5% tolerance.

III. EXPERIMENTAL SETUP

The experimental system under investigation consists of six Rössler oscillators on a ring with diffusive coupling. Each oscillator is represented by the circuit shown in Fig. 1. Applying Kirchhoff's laws and the "golden rules" [14] for the operational amplifiers, this experimental setup can be cast into the form

$$\frac{dx}{dt} = -\alpha(\Gamma x + \beta y + \lambda z),$$

$$\frac{dy}{dt} = \alpha(x + \gamma y), \tag{2}$$

$$\frac{dz}{dt} = \delta\alpha(g(x) - z),$$

where the nonlinearity in the circuit is the piecewise linear function $g(x)$,

$$g(x) = \begin{cases} 0, & \text{if } x < 2.56 \\ \mu(x - 2.56), & \text{if } x \geq 2.56. \end{cases} \tag{3}$$

These equations represent a modified version of the Rössler equations (1), where the quadratic nonlinearity is replaced by $g(x)$ and where the equation for the variable x contains an additional damping term. The parameters in Eq. (2) are determined by the values of the resistors and capacitors in the circuit of Fig. 1 and are given in Table I.

TABLE I. Parameters of the modified Rössler system given by the circuit components.

$\alpha=\frac{R_6}{R_5R_7C_2}$	$\Gamma=\frac{1}{\alpha C_1R_3}$
$\beta=\frac{1}{\alpha C_1R_1}$	$\lambda=\frac{1}{\alpha C_1R_2}$
$\gamma=\frac{R_5}{R_4}$	$\mu=\frac{R_{10}R_{12}}{R_8R_{11}}$
$\delta=\frac{R_5R_7C_2}{R_6R_{12}C_3}$	

This circuit has already been employed in experimental investigations concerning synchronization of oscillators[15] mainly due to the following properties: it is easy to assemble and therefore to reproduce it to have several ''identical'' circuits, it is well behaved in the sense that it presents, besides periodic attractors, just a single chaotic attractor for the explored parameter region. In fact, as control parameter in a single oscillator we chose the parameter μ, which gives the slope of the inclined straight segment for $x \geqslant 2.56$ in the piecewise linear function of Eq. (3). Decreasing the value of the resistor R_{11} ($\mu \propto 1/R_{11}$) we obtain a bifurcation diagram displaying a period doubling cascade to chaos and inside the chaotic regime we see also windows of period 3, 5, 7, etc. In the following analysis we consider two initial behaviors for a single Rössler oscillator: (a) a periodic attractor (period 2) when $R_5=15$ kΩ and $R_{11}=113$ kΩ (typical values), and (b) a chaotic attractor (two small chaotic bands) when $R_5=15$ kΩ and $R_{11}=70$ kΩ (typical values). The trajectories are shown in Fig. 2.

A few comments about the function $g(x)$ defined by Eq. (3) are in order. The replacement of the nonlinearity zx in Eq. (1) by $g(x)$ is very convenient from an experimental point of view since then there is no need for the always troublesome multiplication of two signals, as should be done for the original Rössler system. The piecewise linear function is generated considering an ideal diode, therefore acting as a switch in the circuit. When the diode is in the nonconducting state, $g(x)=0$, and when it is in the conducting state, $g(x)=\mu(x-2.56)$. The value of 2.56 comes out from the fact that we use a silicon diode (considering a breakpoint voltage $V_o=0.69$ V) and that the circuit is fed with a ± 12 V power supply. The abrupt switching model of the diode is not exactly followed in the experiment. Thus, the resulting small quantitative discrepancies between model and experiment may be important when comparing the experimental results with those obtained numerically. We observe a better qualitative agreement between model and experiment for large R_{11} values. In fact, the two initial behaviors considered for a single oscillator ($R_{11}=113$ kΩ and $R_{11}=70$ kΩ) have R_{11} values large enough to support a good qualitative agreement with the numerical analysis. Due to the abovementioned small discrepancies, when we employ in the numerical calculations the same values for R_{11} as those used in the experimental setup we do not reproduce the experimental dynamical behavior. To overcome this drawback we search for different values of R_{11} in the numerical analysis such that the numerical dynamical behavior matches the experimental one. The result is shown in Fig. 2.

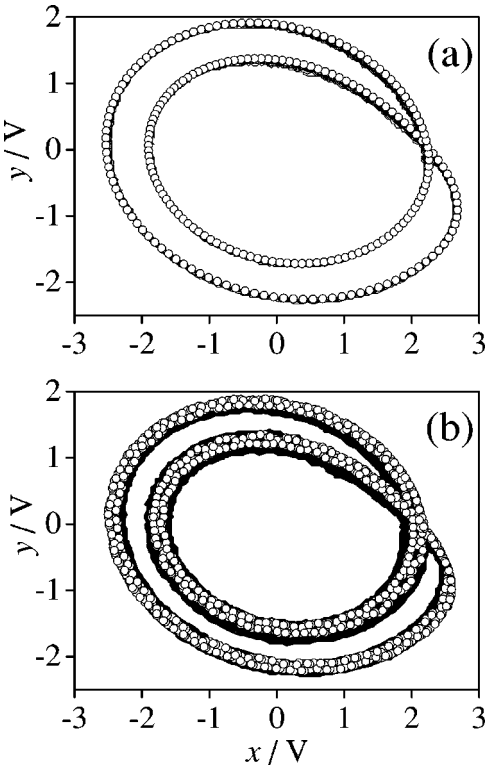

FIG. 2. The black solid lines represent the experimental result for (a) period 2 attractor for a single circuit with $R_5=15$ kΩ and $R_{11}=113$ kΩ, and (b) chaotic attractor for $R_5=15$ kΩ and $R_{11}=70$ kΩ. The white circles represent the corresponding numerical results using for (a) $R_5=15$ kΩ and $R_{11}=150$ kΩ and for (b) $R_5=15$ kΩ and $R_{11}=120$ kΩ.

IV. EXPERIMENTAL RESULTS AND COMPARISON WITH NUMERICAL CALCULATIONS

The oscillators described in the previous section were arranged on a ring with diffusive coupling in three different configurations, or coupling schemes. They are shown in Figs. 3–5 and we call them scheme 1, 2, and 3, respectively. In them the coupling term $-\epsilon(x_{i-1}+x_{i+1}-2x_i)$ is always the same and therefore the group symmetry, D_n, was preserved for all schemes.[4] The difference among them resides in how this signal is injected into each of the six oscillators. The bold arrows in the figures indicate the position where the circuits are modified to produce the desired connection scheme. Throughout the experiment the components R_1, R_2, R_3, R_4, R_6, R_7, R_8, R_9, R_{10}, R_{12}, C_1, C_2, and C_3 were kept constant, independent of the kind of connection of the coupling term.

We proceed now with the experimental study and the numerical analysis of coupling schemes 1, 2, and 3. Our control parameter is the coupling strength ϵ and we adopt the following experimental procedure: beginning from $\epsilon=0$ we increase ϵ smoothly until we reach a synchronization pattern. Regarding the values of ϵ for which the patterns do exist, we observe that each pattern has a basin of attraction, i.e., a pattern may exist for a certain ϵ interval. Then for an ϵ inside the basin of attraction of the pattern into consideration, we

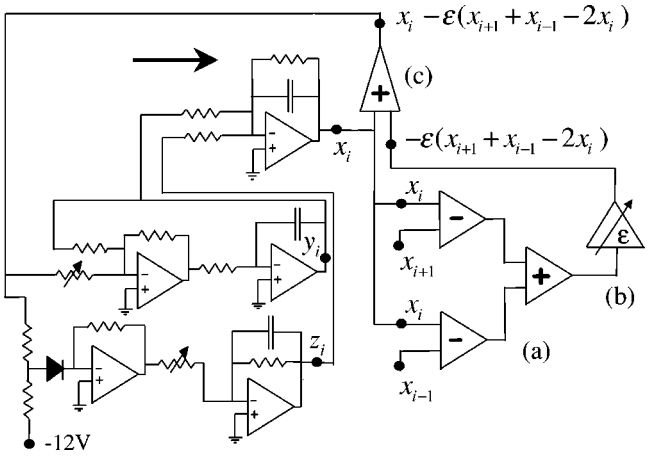

FIG. 3. Coupling scheme 1. For the ith oscillator, in stage (a) the variable x is subtracted from the x values of both nearest neighbors and then the respective results are summed. In (b) this sum is multiplied by the desired coupling strength. Finally in (c) the resulting coupling term is injected into the ith oscillator by subtracting it from the variable x in all equations.

held it constant for the time necessary to perform all measurements to characterize the pattern. Thereafter we keep on increasing ϵ until the next synchronization pattern is established and then proceed in the same way further on. Therefore the initial state for a given measure is, theoretically, that of the pattern observed previously. In this manner we report all experimental synchronization patterns seen for each coupling scheme. The identification of the experimental patterns is done only by visual inspection. We have no *a priori* knowledge of the ϵ values for which there are patterns neither how the stability of the patterns evolve when ϵ is changed. This issue is strongly dependent on the choice of the parameters (R_5 and R_{11}) for each oscillator. Therefore we restrict our investigation to two sets of parameters in the experiment: $R_5 = 15$ kΩ and $R_{11} = 113$ kΩ (periodic evolution for each isolated oscillator) and $R_5 = 15$ kΩ and $R_{11} = 70$ kΩ (chaotic evolution for each isolated oscillator). In order to compare with numerical results we have to take into account that, as already mentioned, there are small quantitative discrepancies between model and experiment. We search for numerical patterns that are dynamically equivalent to the experimental ones. Thus the numerical value of ϵ is not in exact correspondence with the obtained experimentally for a certain pattern.

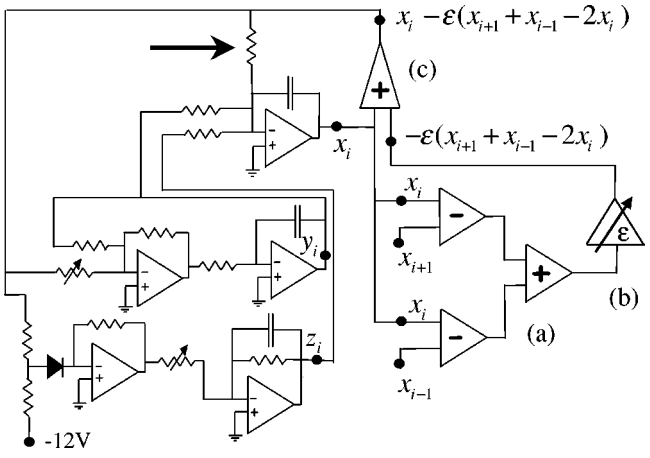

FIG. 4. Coupling scheme 2. The stages (a) and (b) are the same as in Fig. 3. In (c) the coupling term is injected into the ith oscillator by subtracting it from the variable x in the two last equations.

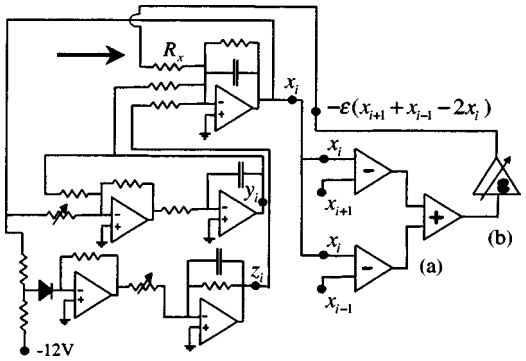

FIG. 5. Coupling scheme 3. The stages (a) and (b) are the same as in Fig. 3. The coupling term is injected into the ith oscillator through resistor R_x by subtracting it from the first equation.

A. Coupling scheme 1

When the oscillators are connected as shown in Fig. 3 the equations representing the system are written as

$$\frac{dx_i}{dt} = -\alpha(\Gamma[x_i - \epsilon(x_{i-1} + x_{i+1} - 2x_i)] + \beta y_i + \lambda z_i),$$

$$\frac{dy_i}{dt} = \alpha([x_i - \epsilon(x_{i-1} + x_{i+1} - 2x_i)] + \gamma y_i),$$

$$\frac{dz_i}{dt} = \delta\alpha(g([x_i - \epsilon(x_{i-1} + x_{i+1} - 2x_i)]) - z_i),$$

$$x_{N+1} = x_1, \quad y_{N+1} = y_1, \quad z_{N+1} = z_1. \tag{4}$$

Setting $R_5 = 15$ kΩ and $R_{11} = 113$ kΩ, the state of the single, noninteracting oscillator is period 2, as shown in Fig. 2(a). In the same figure we show the superposition of the experimental and numerical trajectory. With these initial conditions we have experimentally observed the patterns $\{abcabc\}$ for $\epsilon = 0.25$, $\{abbacc\}$ for $\epsilon = 0.26$, $\{ababab\}$ for $\epsilon = 0.36$ and 0.93, $\{aabaab\}$ for $\epsilon = 0.43$ and 0.46, $\{abcbad\}$ for $\epsilon = 0.58$ and 0.67. A given state of the ring can be analyzed through the graphs generated by plotting the y variable of the ith oscillator versus the y of the jth oscillator (the choice of the y variable is arbitrary, similar results are obtained with x or z). Each plot has its axes labeled with a number i or $j = 1,2,\ldots,6$ identifying each of the six circuits. The lengths of the axes correspond to 3 V (remember that the variables x, y, and z are voltages in the circuit). Oscillators with the same behavior are labeled with a letter (a, b, etc.). The letter associated with each set of identical oscillators is arbitrary; the presence of different labels characterizes a spatial structure in the ring. In Figs. 6(a), 7(a), 8(a), 9(a), and 10(a), we can observe the patterns obtained experimentally. Notice that for some cases the synchronization is quite neat, while in some others, such as Fig. 10(a), it is noisy.

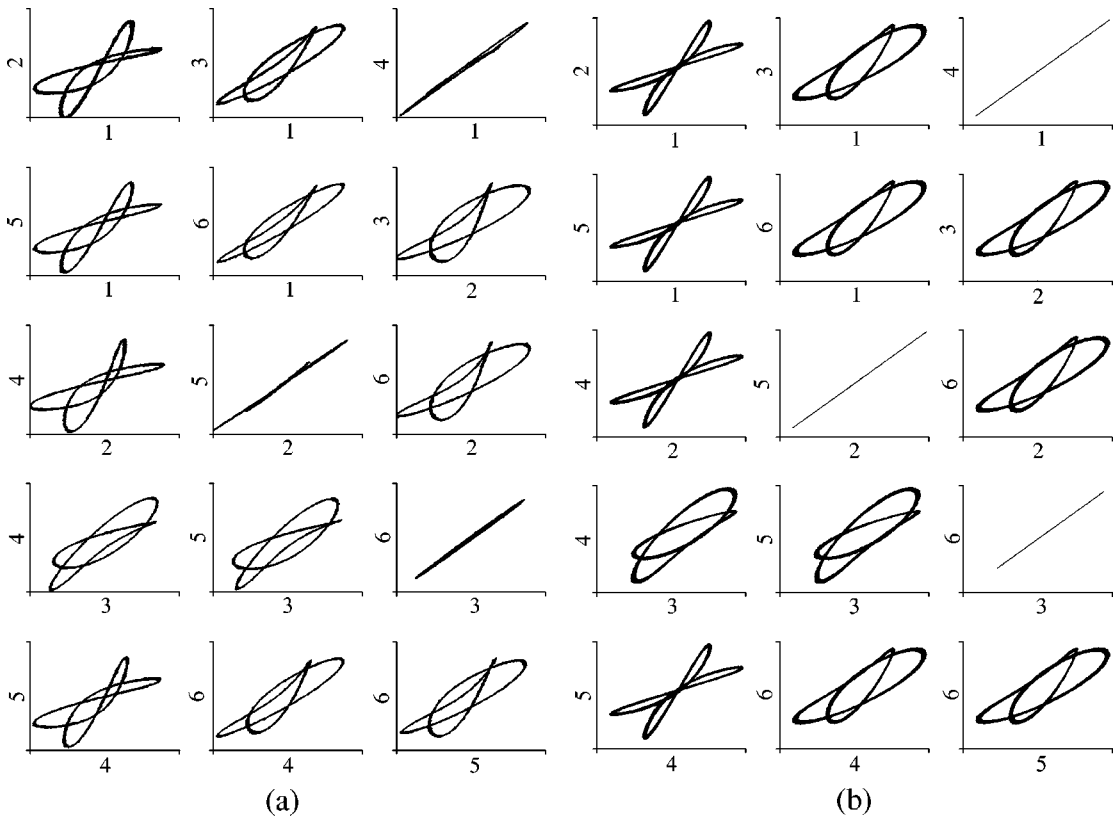

FIG. 6. For coupling scheme 1: (a) experimental $\{abcabc\}$ pattern, $\epsilon=0.25$ and (b) numerical $\{abcabc\}$ pattern, $\epsilon=0.17$. The initial state of a single oscillator is period 2.

A numerical analysis, using Eq. (4) show equivalent states. In Fig. 11 we show the three largest Lyapunov exponents numerically obtained, which helps us to identify whether the evolution of each oscillator in a given pattern is periodic or chaotic. We used $R_5=15\ \mathrm{k}\Omega$ and $R_{11}=150\ \mathrm{k}\Omega$, while the values of ϵ are shown in the corresponding figures. We calculated the Lyapunov exponents in three different modalities: with random initial conditions,

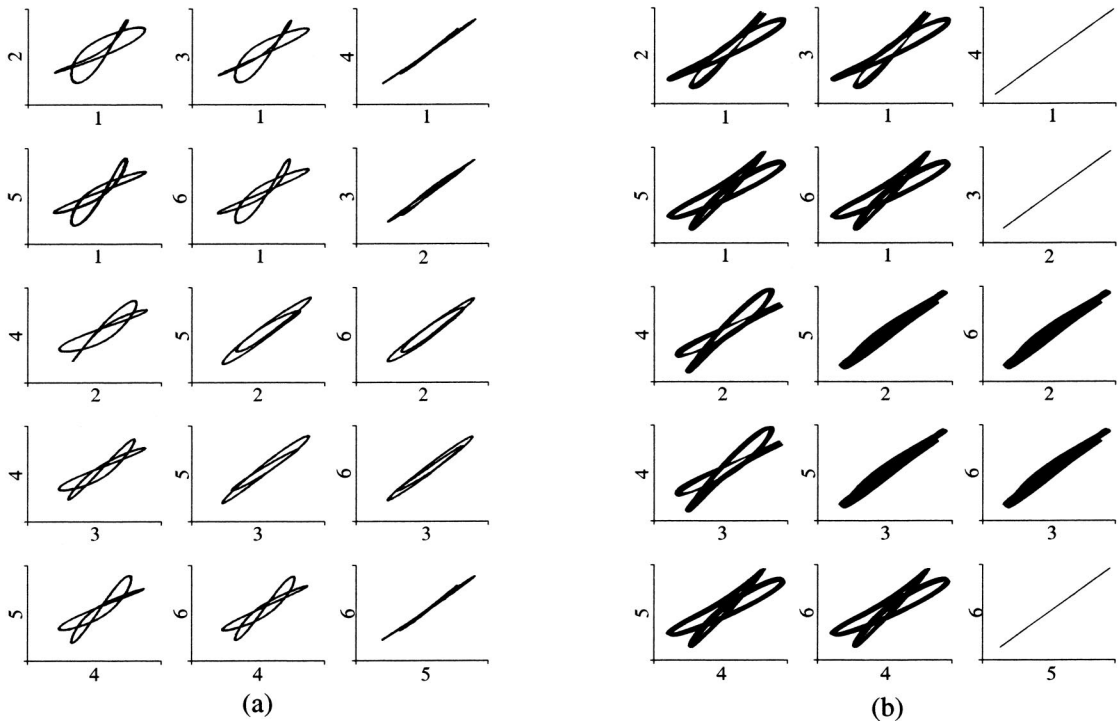

FIG. 7. For coupling scheme 1: (a) experimental $\{abbacc\}$ pattern, $\epsilon=0.26$ and (b) numerical $\{abbacc\}$ pattern, $\epsilon=0.23$. The initial state of a single oscillator is period 2.

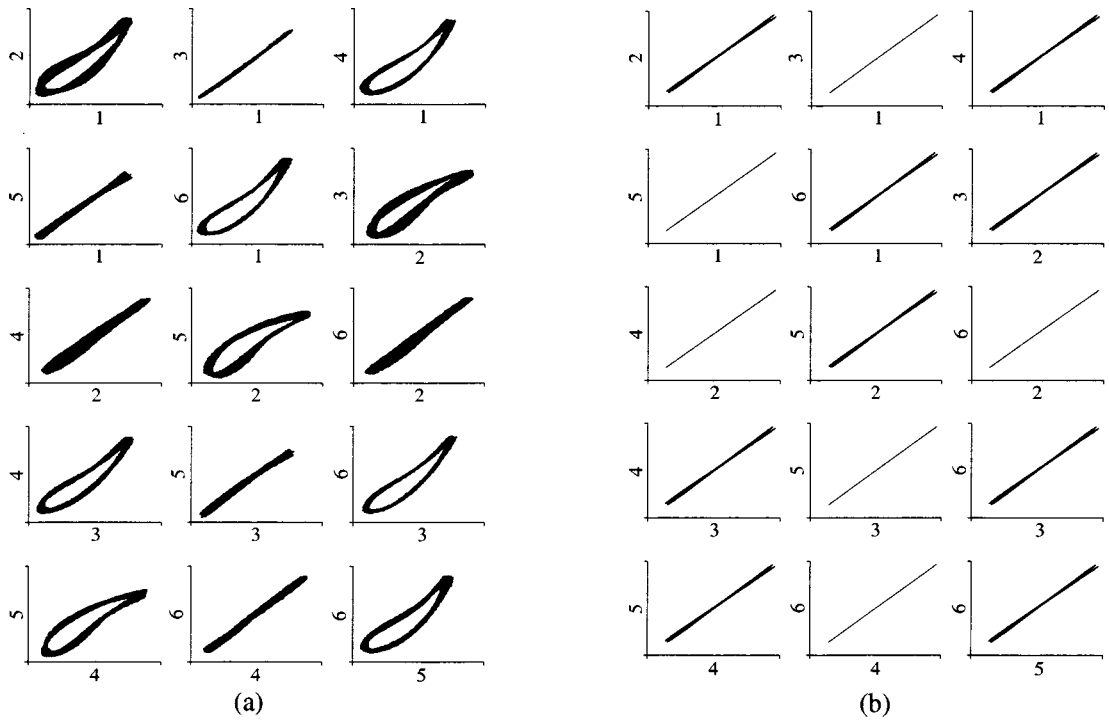

FIG. 8. For coupling scheme 1: (a) experimental $\{ababab\}$ pattern, $\epsilon = 0.36$ and (b) numerical $\{ababab\}$ pattern, $\epsilon = 0.25$. The initial state of a single oscillator is period 2.

starting from the previous state, increasing as well as decreasing the coupling strength. The results are slightly different. As mentioned above, the experimental measurements were taken increasing the interaction strength, while starting from the previous state. Even so, we chose to compare with the calculations made with random initial conditions. The interference with the system while the measurements were performed, cannot guarantee that the evolution of the system has indeed started from the measured pattern. Other sources of inaccuracy are the determination of R_{11} and the function

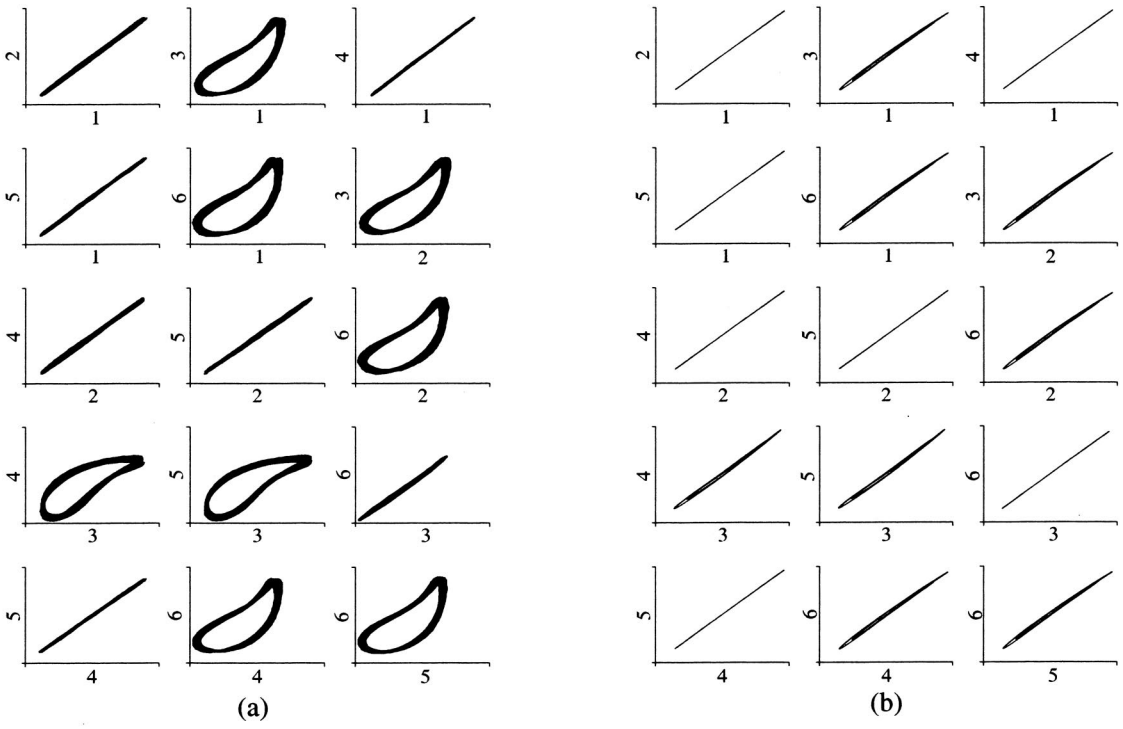

FIG. 9. For coupling scheme 1: (a) experimental $\{aabaab\}$ pattern, $\epsilon = 0.46$ and (b) numerical $\{aabaab\}$ pattern, $\epsilon = 0.48$. The initial state of a single oscillator is period 2.

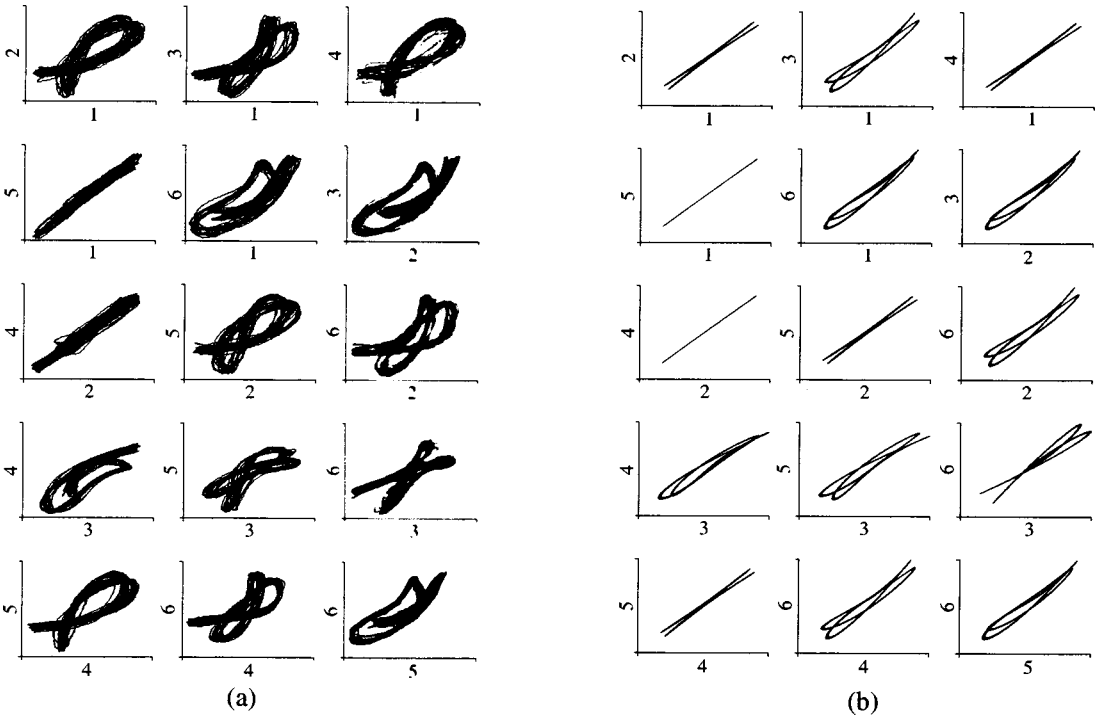

FIG. 10. For coupling 1 scheme: (a) experimental $\{abcbad\}$ pattern, $\epsilon=0.58$ and (b) numerical $\{abcbad\}$ pattern, $\epsilon=0.59$. The initial state of a single oscillator is period 2.

$g(x)$, for which we have used a piecewise linear function, following Heagy *et al.*,[15] and of course the value of the coupling constant.

Comparing the experimental results with the theoretical ones, which are shown side by side in Figs. 6, 7, 8, 9, and 10, respectively (a) and (b), we notice that the similarity of the figures is quite striking. When we compare these results with other patterns where we notice that the resolution is quite good, we may say that the pattern we see is in a partially semisynchronized state. In the case of the patterns $\{ababab\}$ and $\{aabaab\}$, the numerical results have the cluster states a and b very near to each other, and they become difficult to separate. But, the precision of the calculation tells us that they are indeed two clusters.

Then we change the values of $R_5=15\ \mathrm{k}\Omega$ and $R_{11}=70\ \mathrm{k}\Omega$, for which each isolated oscillator is chaotic, the trajectory is shown in Fig. 2(b), together with that calculated numerically for our choice of the nonlinear function $g(x)$. Notice that again they are the same, which allows us to set the values of the parameters for the numerical calculations. The determination of these values is also helped by the graph of the largest Luyapunov exponent (Fig. 11) and the bifurcation diagram, not shown here. In this case we have been able to see experimentally only the pattern $\{ababab\}$ for $\epsilon=0.80$ and full synchronization at $\epsilon=0.56$, which are shown in Figs. 12 and 13, respectively, together with the numerical calculation. For this particular scheme we could say that there is no doubt that the patterns predicted theoretically have been seen experimentally.

B. Coupling scheme 2

For this scheme the point of connection between oscillators is shown in Fig. 4, and the system is determined by the equations,

$$\frac{dx_i}{dt}=-\alpha(\Gamma x_i+\beta y_i+\lambda z_i),$$

$$\frac{dy_i}{dt}=\alpha([x_i-\epsilon(x_{i-1}+x_{i+1}-2x_i)]+\gamma y_i),$$

$$\frac{dz_i}{dt}=\delta\alpha(g([x_i-\epsilon(x_{i-1}+x_{i+1}-2x_i)])-z_i),$$

$$x_{N+1}=x_1,\quad y_{N+1}=y_1,\quad z_{N+1}=z_1. \tag{5}$$

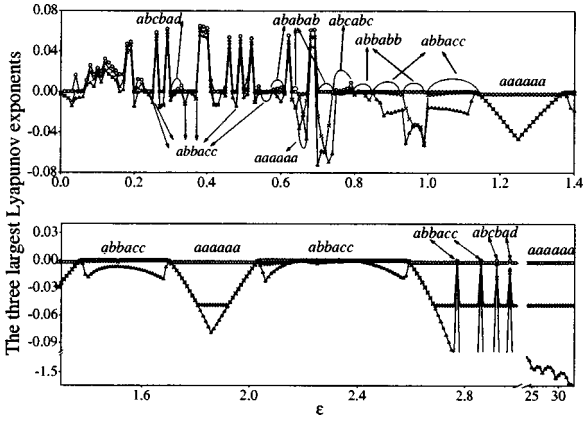

FIG. 11. The three largest Lyapunov exponents for the six oscillators coupled through scheme 1; $R_5=15\ \mathrm{k}\Omega$ and $R_{11}=150\ \mathrm{k}\Omega$.

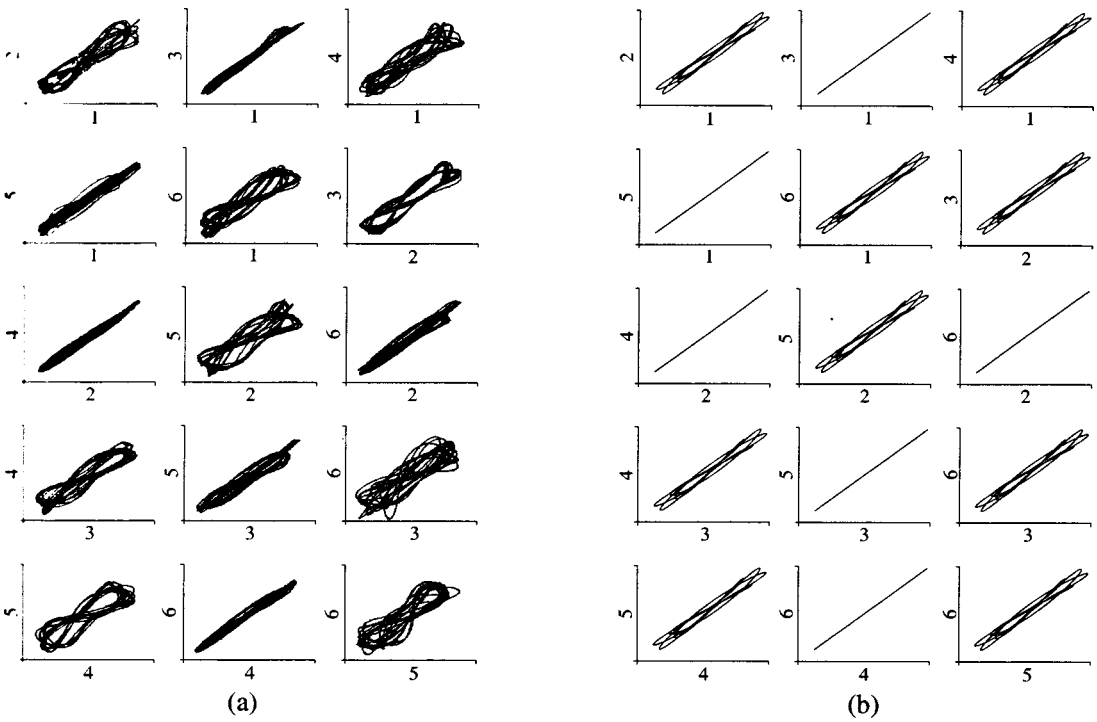

FIG. 12. For coupling scheme 1: (a) experimental $\{ababab\}$ pattern, $\epsilon=0.80$ and (b) numerical $\{ababab\}$ pattern, $\epsilon=0.57$. The initial state of a single oscillator is chaotic.

The values selected for the variable resistors were: $R_5=19.9\ \mathrm{k}\Omega$ and $R_{11}=179.1\ \mathrm{k}\Omega$, which correspond to an initial state of period 2. The patterns observed were $\{abcabc\}$ for $\epsilon=0.13$ and $\{ababab\}$ for $\epsilon=0.56$. They are shown in Figs. 14 and 15, side by side with those calculated numerically. As you can see, again the similarity is large.

C. Coupling scheme 3

We change the structure of the connection in the upper part of the circuit, as seen in Fig. 5, and the connectivity is changed without changing the symmetry of the systems of oscillators. The corresponding equations are

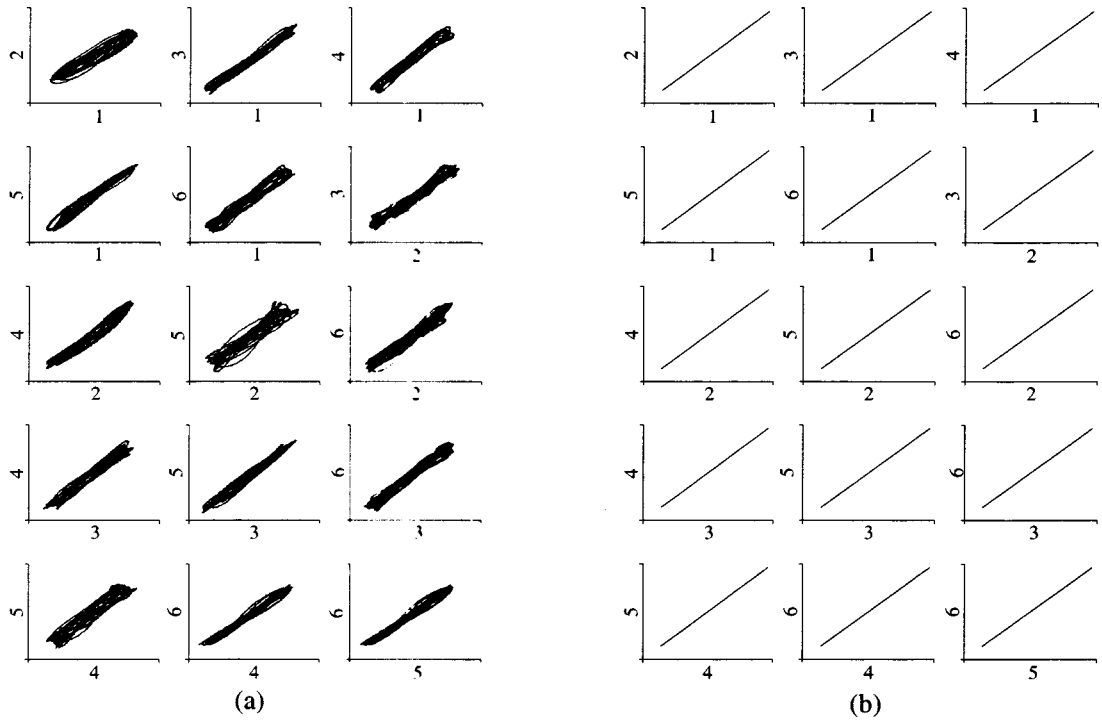

FIG. 13. For coupling scheme 1: (a) experimental $\{aaaaaa\}$ pattern, $\epsilon=0.56$ and (b) numerical $\{aaaaaa\}$ pattern, $\epsilon=0.31$. The initial state of a single oscillator is chaotic.

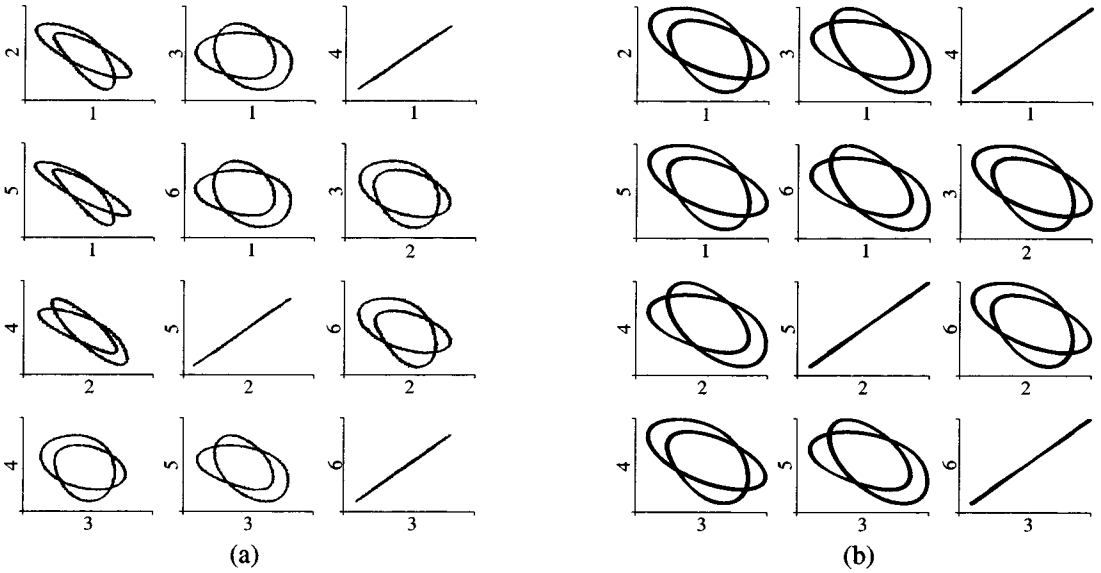

FIG. 14. For coupling scheme 2: (a) experimental $\{abcabc\}$ pattern, $\epsilon=0.13$ and (b) numerical $\{abcabc\}$ pattern, $\epsilon=0.04$. The initial state of a single oscillator is period 2.

$$\frac{dx_i}{dt} = -\alpha(\Gamma x_i + \beta y_i + \lambda z_i) + \eta(x_{i-1} + x_{i+1} - 2x_i),$$

$$\frac{dy_i}{dt} = \alpha(x_i + \gamma y_i),$$

$$\frac{dz_i}{dt} = \delta\alpha(g(x_i) - z_i),$$

$$x_{N+1} = x_1, \quad y_{N+1} = y_1, \quad z_{N+1} = z_1. \tag{6}$$

In this setup the coupling constant is given by $\eta \equiv \epsilon / C_1 R_x$, where the coupling resistor has the value $R_x = 100\ \text{k}\Omega$. The values selected for the variable resistors were $R_5 = 15\ \text{k}\Omega$ and $R_{11} = 70\ \text{k}\Omega$, for which each isolated oscillator is chaotic. In this case no patterns were observed except full synchronization for $\epsilon = 0.4$ and above. Since this case is the most obvious one, we are not showing it here. We believe the low value of the coupling constant to be the main reason for not finding partial synchronization, since in that region the

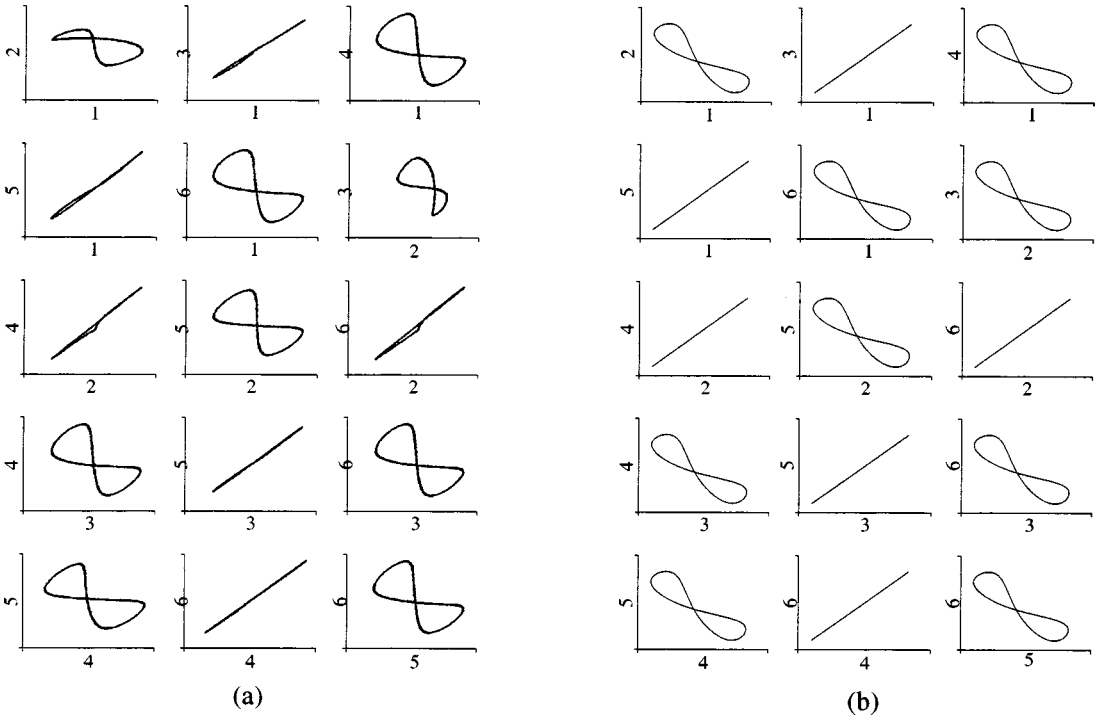

FIG. 15. For coupling scheme 2: (a) experimental $\{ababab\}$ pattern, $\epsilon=0.56$ and (b) numerical $\{ababab\}$ pattern, $\epsilon=0.15$. The initial state of a single oscillator is period 2.

noise masks most of the measurements. The experimental data do not compare with the fully resolved patterns presented in the other schemes.

V. CONCLUSION

In conclusion, we have presented experimental evidence of the existence of partial synchronization in a system of coupled circuits, modelled by Rössler oscillators. The circuits are placed in a ring with symmetric nearest neighbor interaction, corresponding to the D_n symmetry described by Golubitsky *et al.*[4] All the allowed patterns for the given symmetry have been seen experimentally, when the system starts with the individual circuits in a periodic state. We have seen only some of the patterns when starting in the chaotic state. In both cases, when increasing ϵ, numerically we find a major number of ϵ intervals corresponding to partial synchronization than in the experiment. In part this is due to small discrepancies between the experiment and the model, which also account for the inexistence of an exact coincidence of the value of ϵ for an experimentally seen pattern and a numerically calculated one. Nevertheless it was possible to find numerically patterns that are dynamically in good qualitative agreement with the experimental ones such that, regarding their ϵ values, they are ordered in the same way. We believe that the main cause for not finding some allowed patterns in the experiment is due to the noise always present in an experiment and that was not considered in the numerical analysis. When the coupling term is summed to the x variable (coupling schemes 1 and 2), then even a very small amount of noise plays an important role as it may be amplified by the nonlinear function $g(x)$. Besides the noise, the inaccuracy in the determination of the parameters as well as $g(x)$ are also responsible for the lower number of experimental patterns compared to those calculated numerically. Furthermore we have also to consider that some patterns may coexist with other stable patterns and that they usually have small basins of attraction. Therefore these patterns certainly are difficult to be found experimentally. For numerical simulation we can always find them by properly choosing the initial conditions, but for experiments the initial conditions cannot be well controlled. In spite of this, we have shown the existence of partial synchronization both in the periodic as well as in the chaotic regime, but we believe, further experiments, with a more accurate setup, should be used to fine tune the scanning.

ACKNOWLEDGMENTS

T.B. acknowledges the Brazilian agency FAPERGS for support, and the hospitality of ICTP at Trieste, Italy during a one month stay. I.A.H. thanks the Brazilian agency CNPq for support.

[1] J.F. Heagy, L.M. Pecora, and T.L. Carroll, Phys. Rev. Lett. **74**, 4185 (1995).
[2] G. Hu, Y. Zhang, H.A. Cerdeira, and S. Chen, Phys. Rev. Lett. **85**, 3377 (2000).
[3] Y. Zhang, G. Hu, and H.A. Cerdeira, Phys. Rev. E **64**, 037203 (2001).
[4] M. Golubitsky, I.N. Stewart, and Dg. Schaeffer, *Singularities and Groups in Bifurcation Theory* (Springer Verlag, New York, 1988); P.L. Buono, M. Golubitsky, and A. Palacios, Physica D **143**, 74 (2000).
[5] J.J. Collins and I. Stewart, Biol. Cybern. **68**, 287 (1993).
[6] S. Strogatz, Physica D **143**, 1 (2000).
[7] L. Ren and B. Ermentrout, Physica D **143**, 56 (2000).
[8] V.N. Belykh, I.V. Belykh, and M. Hasler, Phys. Rev. E **62**, 6332 (2000).
[9] Y. Zhang, G. Hu, H.A. Cerdeira, S. Chen, T. Braun, and Y. Yao, Phys. Rev. E **63**, 026211 (2001).
[10] M. Ding and W. Yang, Phys. Rev. E **54**, 2489 (1996).
[11] J. Yang, G. Hu, and J. Xiao, Phys. Rev. Lett. **80**, 496 (1998).
[12] Y.L. Maistrenko, V.L. Maistrenko, A. Popovich, and E. Mosekilde, Phys. Rev. E **57**, 2713 (1998); Phys. Rev. Lett. **80**, 1638 (1998); Phys. Rev. E **60**, 2817 (1999).
[13] G. Hu, F. Xie, Z. Qu, and P. Shi, Commun. Theor. Phys. **31**, 99 (1999).
[14] P. Horowitz and W. Hill, *The Art of Electronics* (Cambridge University Press, Cambridge, 1980).
[15] J.F. Heagy, T.L. Carroll, and L.M. Pecora, Phys. Rev. E **50**, 1874 (1994).